TRR
JOURNAL OF THE TRANSPORTATION RESEARCH BOARD

Article

Transportation Research Record
1–10

DOI: 10.1177/0361198118787975
journals.sagepub.com/home/trr
SAGE

Effect of Synthetic Fiber State on Mechanical Performance of Fiber Reinforced Asphalt Concrete

Hossein Noorvand[1], Ramadan Salim[1], Jose Medina[1], Jeffrey Stempihar[1], and B. Shane Underwood[1]

Abstract

It has been recognized that there exists a potential benefit from using synthetic fibers to reinforce asphalt mixtures. In these mixtures, the state of the fibers may play an essential role in their reinforcement function. This study aims to quantify the state of synthetic fiber distribution for two different aramid fiber–based asphalt mixtures and then show the impacts of fiber dispersion on modulus, rutting, and fatigue performance of each asphalt mixture in comparison with one another and with respect to an equivalent non-reinforced asphalt mixture. Both a quantitative and qualitative assessment of aramid fibers distribution as well as state of fiber are investigated using a fiber extraction procedure and microscopy imaging, respectively. The results suggested that a higher level of micro-fibrillation as well as high distribution of aramid fibers improved the rutting resistance of asphalt mixtures, while the distribution level of aramid fibers and fibers state did not affect the modulus and fatigue. These results are specific to the mixture studied but provide the first objective and detailed study describing fiber state, fiber dispersion, and performance.

The use of reinforcing fibers in asphalt concrete (AC) has been documented in many studies (*1, 2, and the citations therein*). Some of these studies have shown that the addition of fiber in dense graded and open graded AC mixtures can change the dynamic modulus and phase angle of the mixture (*3*), relaxation ability and rutting resistance (*4–6*), and resistance to low-temperature cracking, fatigue cracking, and reflective cracking (*6–9*). More than half of state agencies in the United States use fibers in AC mixtures (*1*), but most use non-synthetic fibers to reduce drain down in open graded and stone mastic asphalt mixtures. Fibers commonly used for this purpose include cellulose, mineral fibers, and other plant-based materials. Synthetic polymeric fibers (i.e., polypropylene, polyester, aramid, and nylon), glass fibers, and recycled fibers are also used for the purposes of providing mechanical reinforcement and improving rutting and cracking in AC, referred to generically as mechanically fiber reinforced asphalt concrete (M-FRAC) (*1*).

Most studies in this area attempt to experimentally observe the effect of different fiber types on traditional mechanical measures. Previous studies have used indirect tensile tests, pull out tests, repeated load permanent deformation tests, triaxial shear strength tests, and uniaxial fatigue tests to quantify the benefits of synthetic fibers (*3, 6–8*). While published studies generally demonstrate positive benefits from using M-FRAC, it is not always the case, and when improvements are found they vary with respect to the types of fibers and the particular study (*10*, *11*).

One possible reason for this inconsistency may be a lack of understanding in the basic, fundamental mechanisms that govern the mechanical response of these mixtures and the effect of fiber state with respect to these mechanisms. The essential role of synthetic fibers in M-FRAC is to act as reinforcement elements to enhance the tensile properties of the mixture, and the mechanisms that dictate their effectiveness are how easily the fibers pull out from the asphalt mastic and how easily the fibers break (*12*). Both mechanisms, and their ultimate effect on the composite performance are related to the specific state of fibers in the mixtures. The fiber state, inclusive of how the fibers are dispersed, where the fibers are located, and surface morphology directly affect these mechanisms. These effects have been recognized in previous studies, but little to no systematic study has been done to attempt to quantify and correlate the effect of fiber state to the performance improvements.

[1]Ira A. Fulton Schools of Engineering, School of Sustainable Engineering and the Built Environment, Arizona State University, Tempe, AZ

Corresponding Author:
Address correspondence to B. Shane Underwood:
shane.underwood@ncsu.edu

Objective

The specific objectives of this study are to measure the mechanical properties of two M-FRAC specimens with synthetic aramid fibers in different states, then to quantify the state of aramid fiber distribution in AC, and finally to examine the impacts of aramid fiber dispersion on laboratory modulus, rutting, and fatigue performance of asphalt mixtures.

Methodology

The experimental approach involved first conducting mechanical tests to evaluate the response and laboratory performance of M-FRAC mixtures and then evaluating the dispersion, distribution, and morphology of fibers.

Materials

A 12.5 mm Marshall mixture (PG 70-10, 5.2% binder) from Tucson, Arizona was used for this study. A total of three variations to this plant-produced mixture were used in this study: a non-reinforced mixture (control), a M-FRAC mixture with overall good dispersion of synthetic fiber (FA), and a M-FRAC mixture with overall poor dispersion of synthetic fiber (FB). Both M-FRAC mixtures contained synthetic aramid fibers at a dosage of 65.5 g per tonne of mix. The aramid fibers were 19 mm long and were introduced in bundles of approximately 3,000 individual fibers each. The fibers have a reported tensile strength between 2,700 and 3,000 MPa and are not affected by temperatures up to 426°C.

In the field, both fiber mixtures were added directly into the hot aggregates in the drum just before the application of hot binder at the dust port. Both manufacturers' products were added with the addition of forced air. Also, the fibers were mixed with hot aggregates for a few seconds before adding the hot binder. Differences in dispersion and distribution are achieved due to the use of different technologies in FA and FB. In FA, the aramid fibers are introduced along with polyolefin fibers while in FB the aramid fibers are coated in a thin membrane of wax, which melts as the fibers are mixed in. Theoretically, both FA and FB try to deliver fibers into the mixing process with high aspect ratios (ratio of diameter to length) so that early in the mixing process they distribute better and do not interfere with the process. Both technologies then rely on the fibers separating and dispersing throughout the mixture in a low aspect ratio state so that more volume of the mixture can be reinforced. In FA, the polyolefin fibers facilitate this transition by first carrying aramid bundles throughout the mixture. Then, as the polyolefin fibers melt they change shape to help pull aramids away from the bundles and also act to neutralize static charges that can cause aramids to agglomerate into cotton-ball-like structures. Aramids may also be dispersed by frictional forces between the aramid fibers and the aggregate. In FB, the wax keeps the aramids bundled until it melts, at which point the aramids are dispersed through frictional forces between the fibers and the aggregate. It is not known if the wax completely melts into the asphalt mixture or if as it melts it seeps deeper into the bundle so that dispersing the fibers requires continual agitation.

At the laboratory, the mixtures removed from the 19 L metal pail as received by heating them at 135°C for 90 minutes, and then samples were randomly taken from multiple pails. Also, representative samples from each mix were selected to perform extraction to check the equivalency of the gradation and binder content of the mixes so that any differences in the performance of the mixes could be attributed to differences in the fiber state. On average, the difference in percent passing on sieve sizes greater than 4.75 mm and less than 4.75 mm between the mixes was less than 2% and 0.5%, respectively. The binder content and the theoretical maximum specific gravities (Gmm) from the extraction were consistent across all three mixtures. Also, the Gmm of the mixtures was within the difference of two samples limit stated in AASHTO T209. Based on the results, the three mixtures appear to be consistent, with the exception that FA and FB mixtures contain fibers.

Mechanical Characterization

In total, three different mechanical experiments were conducted: dynamic modulus test, repeated load permanent deformation test, and uniaxial fatigue test. The target air void level for all tests was 5.5 ± 0.5%, which was the target air void content of the overlay surface course for the project. All specimens were compacted with the gyratory compactor, 150 mm in diameter and 170 mm in height. Specimens were then cut and cored to their final geometry.

Dynamic Modulus Test. Temperature and frequency sweep tests were performed per AASHTO T342 protocol except that the temperatures tested were 4.4, 21.1, and 37.8°C. Tests were performed on cylindrical specimens, 100 mm in diameter and 150 mm in height, and before testing they were instrumented with three linear variable displacement transducers (LVDTs) spaced at 120° intervals on the specimen surface. The readings from these LVDTs along with the applied forces were used to compute dynamic modulus, $|E^*|$, and phase angle, δ, at each test condition.

Repeated Load Permanent Deformation Test. The repeated load permanent deformation, also known as flow number test, was performed to evaluate the permanent deformation characteristics of the asphalt mixtures. The test procedure followed that specified in AASHTO TP79. The test was conducted under atmospheric conditions, a stress level of 160 kPa, and at 50°C. Three replicates were tested for each mixture. Tests were carried out on cylindrical specimens, 100 mm in diameter and 150 mm in height. The deformations were measured using LVDTs mounted to the surface of the sample.

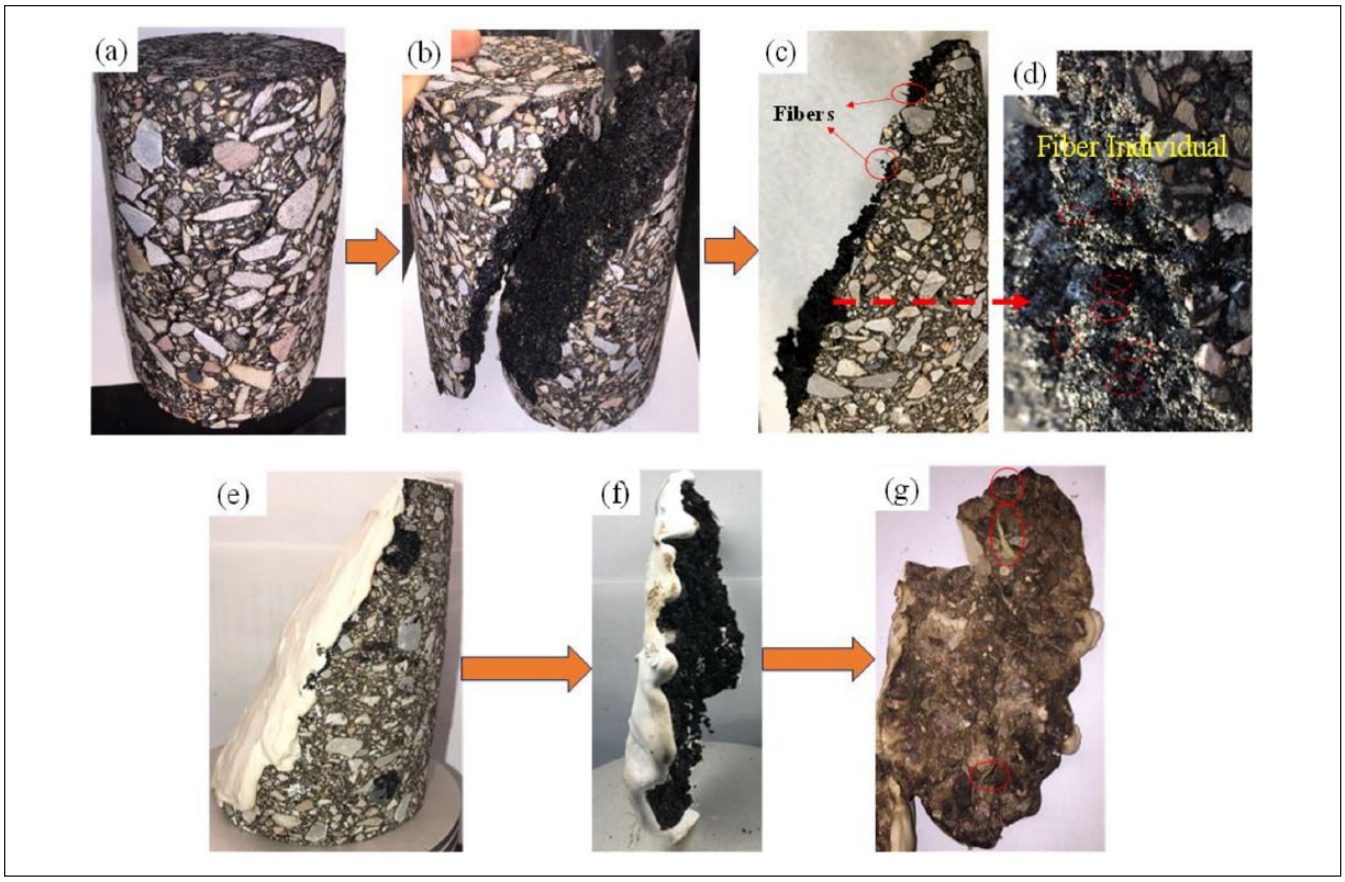

Figure 1. Summary of casting method to evaluate in-situ fiber state: (*a*) tested specimen, (*b*) splitting specimen along the diagonal, (*c*) half splitting specimen, (*d*) zoomed in photo of region identified in (*c*), (*e*) casting on split specimen, (*f*) separated asphalt mixtures from cast specimen, and (*g*) complete separation of asphalt mixture from cast specimen.

Uniaxial Fatigue Test. The uniaxial fatigue test was performed per AASHTO TP107 with the exception that the test specimens were 75 mm in diameter and 150 mm in height. A sinusoidal deformation along the long axis of a cylindrical test specimen is repeated until it fails. Tests were conducted in controlled actuator displacement mode at 10 Hz loading and 18°C. On-specimen measurements of displacement were recorded along with the applied load throughout the test. As per AASHTO TP107, the result of the test is a damage characteristic function used to predict the fatigue life of AC (*13*).

Fiber State

The state of the fibers is described based on three parameters: dispersion, distribution, and surface morphology. Dispersion refers to the process whereby the fiber bundles added to the mixture are dispersed in the mixture. Distribution represents how the dispersed fibers are spatially located through the mixture. Surface morphology characterizes the form and shape of fibers present in the mix.

Fiber Extraction. To evaluate dispersion, aramid fibers were extracted using a procedure developed at Arizona State University (ASU) (*14*), which is essentially the same as ASTM D2172 except that attention is given to observing, separating, and cleaning the fibers in the mixture after soaking the mixture and centrifuging off the solvent. The centrifugal extraction process has two limitations: (1) it can alter the state of the fibers, but studies at ASU (not shown here) reveal that the effect is generally negligible and does not alter the characteristics to a quantifiable amount and (2) separating and cleaning all individual fibers is tedious and time consuming, and in practice a grouping of 3–10 individual fibers (defined as a very small cluster) may be counted as individuals instead of clusters. The ASU test method describes the state of dispersed aramid fibers in AC as one of four conditions: bundles, agitated bundles, clusters, and individuals. A bundle is the condition of the fibers as supplied by the manufacturer (before introduction to AC). Their existence in the final mixture is undesirable as it indicates zero dispersion of the fibers. With only a little agitation, these bundles disperse some of the fibers, but the resulting agitated bundles may still be visibly similar to the original bundles. With sufficient agitation, the fibers will individually disperse throughout the mixture. These individual fibers are the most desirable condition since their existence suggests the formation of a

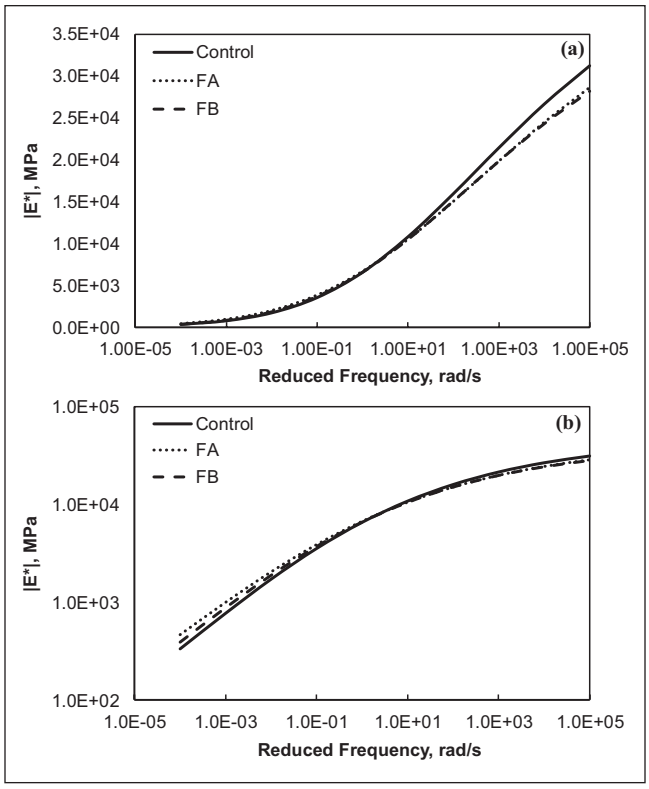

Figure 2. Comparison of |*E**| master curves in: (*a*) semi-log scale and (*b*) log-log scale.

fibrous network throughout the mixture. As the condition transitions between agitated bundles and individuals, the fibers may form loosely connected clusters that provide a dense network in a relatively small volume of material.

After the asphalt binder is extracted, the fibers are separated into the aforementioned categories and the total aramid dosage rate is determined along with the relative proportions of fibers in each category. Of principal interest is the proportion of fibers in the individual state and Equation 1 defines the ratio that quantifies this proportion, known as aramid dispersion state ratio (*ADSR*). A larger *ADSR* signifies the existence of more fibers in the individual state. Supplemental calculations for fibers in the cluster and agitated bundle states are also performed. A test result is reported based on the average of two individual centrifugal extractions.

$$ADSR = F_I = \frac{M_I}{M_a} \times 100 \quad (1)$$

where;
F_I = fibers in the individual state (%),
M_I = fibers in the individual state (g), and
M_a = total extracted mass before separation (g).

Failure Surface Casting. Castings of the failure surface of tested specimens were made to observe the distribution of the aramid fibers throughout the asphalt mixture. The process is performed on mechanically tested specimens shown in Figure 1*a*. First, mechanical test samples are heated to 60°C for 30 minutes and split along a diagonal line extending from the lower edge of the specimen to the upper opposite edge so that fiber orientations could be viewed with respect to both the horizontal and vertical directions, Figure 1*b*. Although the different dispersion states are evident on the surface of the split samples, Figure 1*c* and *d*, detailed comparisons are not possible because the fibers are coated with asphalt and hard to see. So, a thin layer of fluid plaster is poured on the fracture surface of samples and embed the surface fibers. Once the casting cures, Figure 1*e*, the samples are heated to 80°C to carefully separate as much mixture from the cast as possible, Figure 1*f*. Then the remaining samples are soaked in solvent to dissolve the asphalt and completely remove all remnants of the test specimen from the casting. Finally, photos are taken of the surface and evaluated, Figure 1*g*.

Microscopy Imaging. Original and extracted fibers were imaged using a Philips SEM-XL30 Environmental FEG scanning electron microscope (SEM) under the following conditions: environmental mode, secondary electron signal, and accelerating voltage of 15 kV. Fibers were also sputter coated with gold for 2 minutes to improve the electrical conductivity and resolution of the images.

Results

Mechanical Characterization

Dynamic Modulus Test. Data from the |*E**| experiment is presented in the form of dynamic modulus master curves in Figure 2. The dynamic modulus data are shown in both log-log and semi-log scales so that any differences in the moduli at high and low temperatures, respectively, can be observed. It is seen that the moduli values for all three mixtures are very similar at the intermediate temperature. However, at lower temperatures (higher reduced frequencies) the mixes with aramid fibers yield lower moduli values and at higher temperature (lower reduced frequencies) they yield higher moduli. At these higher temperatures, the FA mix exhibits slightly higher average values than the FB mix. ANOVA and statistical *t*-test analyses were performed at a 95% confidence level. The ANOVA analysis was used to compare the difference between all means and evaluate the significance of the total differences and the *t*-test was performed to compare individual cases to the control mixture and individually between the fiber mixes. In all cases, the results indicated a lack of statistical significance in the moduli. Thus, while on-average differences are evident these effects are not significant.

Repeated Load Permanent Deformation Test. Figure 3 shows the accumulated permanent strain during the repeated load

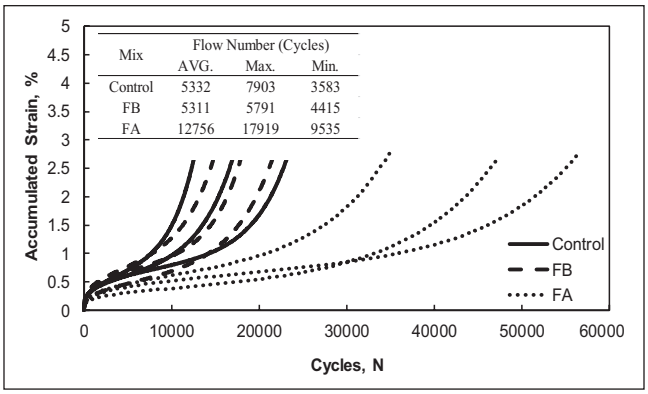

Figure 3. Accumulated strain during flow number test.

permanent deformation test for each of the mixtures. The resulting flow number values from this analysis are also shown as a tabular inset into this figure. Figure 3 shows that the FB and control mixture exhibit similar permanent strain response under the repeated loading, but that the FA mixture accumulates strain at a slower rate and undergoes more repetitions before reaching the onset of flow. In fact, the FA mixture exhibits an increase in average flow number of 139% compared with the control and FB aramid mixtures.

Axial Fatigue Test. The damage characteristic curve for the samples tested in this task is shown in Figure 4*a* for control, FA, and FB. These curves show that mixes with fibers have damage curves that are very similar to those of the control mixtures. These damage curves are fit to the analytical expression shown in Equation 2 and then used with Equation 3 to predict the fatigue life of the mixtures. More details on the analytical process to characterize the damage functions and to predict the number of cycles to failure can be found elsewhere (*13*). Figure 4*b* shows the failure envelopes for each mix type for constant strain–based analysis, which shows that the fiber reinforced samples have approximately twice the fatigue life at a fixed strain level with the FA mixture being slightly better than FB.

$$C = 1 - C_1 S^{C_2} \tag{2}$$

$$N_f = \frac{(f_{red})(2^{\alpha})\left(\frac{(1-C_f)}{C_1}\right)^{\frac{(\alpha-\alpha C_2+1)}{C_2}}}{(\alpha-\alpha C_2+1)(C_1 C_2)^{\alpha}\left[(\varepsilon_{0,pp})(|E^*|)\frac{\beta+1}{2}\right]^{2\alpha} K_1} \tag{3}$$

where;

C = pseudostiffness,
S = internal state variable to quantify damage,
C_1,C_2 = fitting coefficients,
N_f = predicted number of cycles to failure,
f_{red} = reduced frequency for the simulation condition, and
α = damage accumulation rate,
C_f = stiffness ratio at failure,
$\varepsilon_{0,pp}$ = peak-to-peak strain amplitude,
|E*| = dynamic modulus at the simulation condition,
β = wave shape factor (taken as 0 for this study), and
K_1 = loading shape factor (*13*).

Fiber State

Quantity and Condition of Aramid Fiber after Extraction 41. Table 1 summarizes the extraction results first in terms of the aramid dosage rate, which is simply the mass of the aramid fiber with respect to the total weight of the mixture. Both FA and FB contained similar dosage levels (within approximately 8% of one another) and were within 1% to 5% of the target rates (recall that the target fiber dosage rate was 65.5 g/tonne). The difference between replicates was higher in the FB mixture than the FA mixture. Also, the percentages of each of fiber states (*ADSR*, agitated bundles, and clusters)

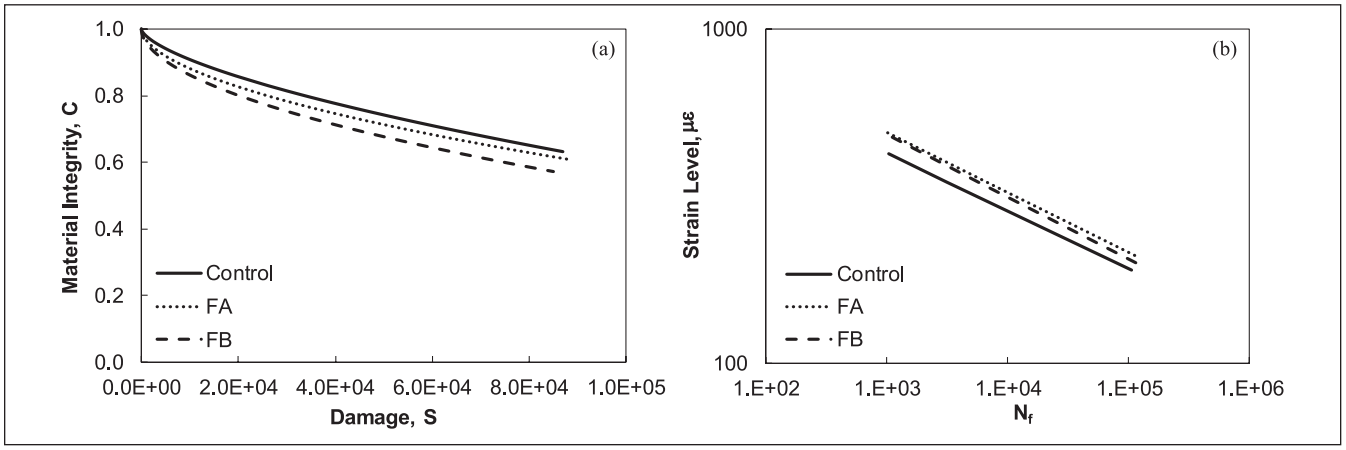

Figure 4. Results of fatigue evaluation: (*a*) damage characteristic curve and (*b*) predicted fatigue life relationships.

Table 1. Summary of Extracted Aramid Dosage and Fiber State

Specimen ID	Aramid dosage rate (g/tonne)/(oz/ton)	State of aramid (%)		
		Agitated bundle	Cluster	ADSR (individual)
FA-1	68.7/2.2	2.0	8.0	90.0
FA-2	65.6/2.1	0.0	13.0	87.0
Average FA	67.1/2.15	1.0	10.5	88.5
FB-1	50/1.6	69.0	12.0	19.0
FB-2	96.8/3.1	78.0	9.0	13.0
Average FA	71.8/2.3	73.5	10.5	16.0

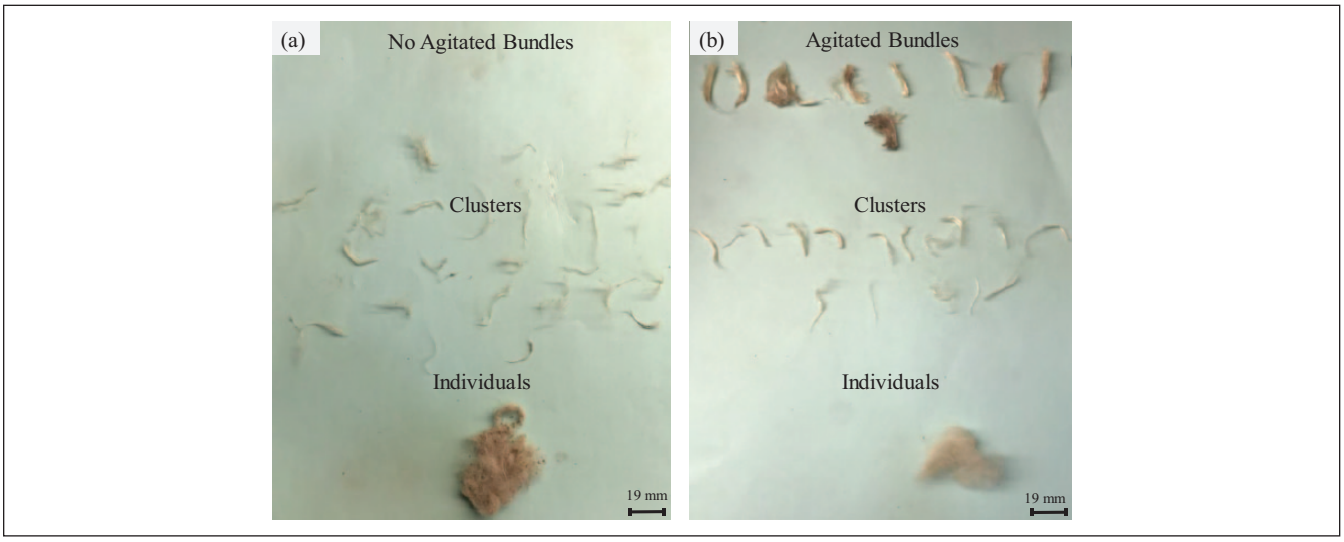

Figure 5. State of extracted aramid fibers from a single sample of (*a*) FA and (*b*) FB.

were determined. The FA mixtures had an average *ADSR* value of 88.5% while FB mixtures had an average *ADSR* of 16%. In the FB case, most of the fibers are dispersed in the agitated bundle condition (73.5% on average). These findings provide some support for the variation observed in the dosage rates of FB replicates because agitated bundles can lead to larger differences in sample-to-sample aramid mass since one or two additional or fewer bundles can alter the mass substantially.

Figure 5 also shows the clear difference between state of the fibers in the FA and FB mixtures after extraction. Figure 5*a* shows that only individuals and clusters exist in FA, and Figure 5*b* shows the presence of agitated bundles in FB and a much lower proportion of individuals than FA. It is important to mention that for the individual fibers the extraction and cleaning process result in the cotton-ball-like agglomeration as seen in these figures. This structure in no way represents how the individual fibers exist in the mixture.

Qualification of Distribution of Aramid Fibers. Images of the castings from the internal diagonal planes of both FA and FB mixtures are shown in Figures 6 and 7. A best effort was made to clearly capture fibers in each photo, and for further clarity of the fibers' state and location, the images were modified with stars, circles, and squares to show locations of fibers in the form of individuals, clusters, and bundles, respectively. A part of the photos in Figures 6*a* and 7*a* was enlarged to more clearly show the existence of individual fibers, as seen in Figures 6*b* and 7*b*. Overall, as the *ADSR* values suggest, a substantially greater number of individual fibers was observed in the casting of the FA mixture (Figure 6). Conversely, the casting of FB yielded a considerably greater number of agitated bundles (Figure **7**). Additionally, it was recognized that individual fibers were evenly distributed throughout both FA and FB and they were oriented in all directions (horizontal, diagonal, and vertical). In this study, no attempt was made to quantify the relative proportion of individual fibers oriented in each direction, but it was observed that a larger proportion of the individual fibers were oriented with their long axis perpendicular to the compaction and testing direction.

With respect to distribution and orientation of bundles and clusters, it was observed that clusters and bundles were mostly distributed and located toward the edges of samples

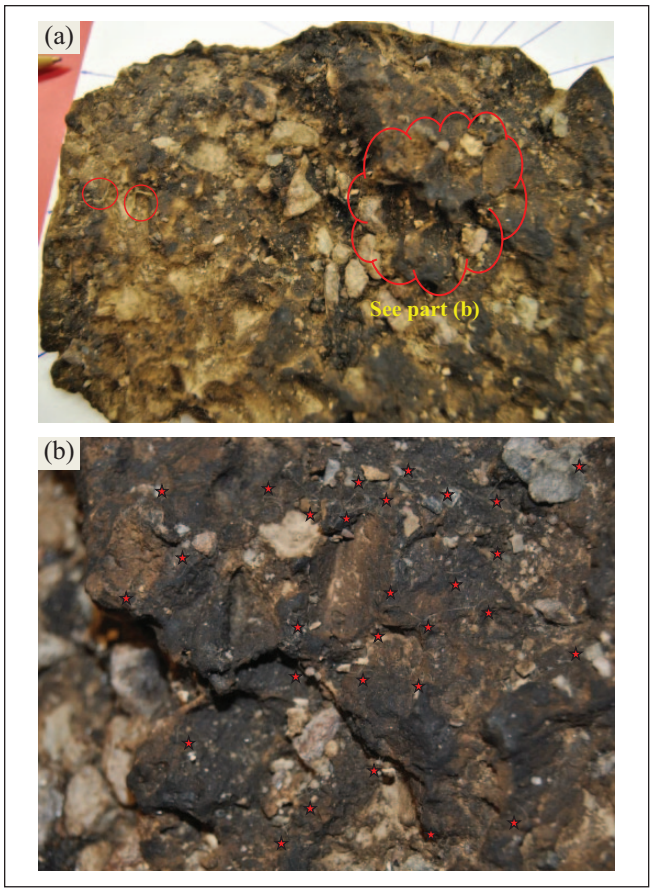

Figure 6. Photos taken from the aramid fibers distributed on the surface fracture of each FA mix: (*a*) overall view of casting surface and (*b*) enlarged photo of central section.

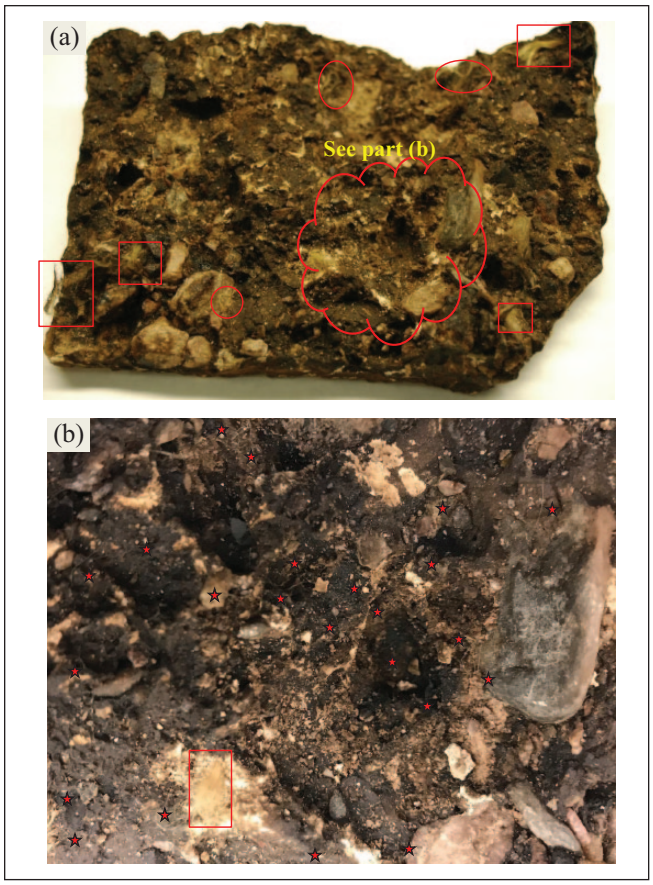

Figure 7. Photos taken from the aramid fibers distributed on the surface fracture of each FB mix: (*a*) overall view of casting surface and (*b*) enlarged photo of central section.

and oriented either horizontally or vertically, unlike individual fibers that tend to be oriented mostly horizontally. It should be noted that the location of clusters and bundles toward the edges of the samples observed in this study might not necessarily be interpreted as the distribution behavior of clusters or bundles. Rather it could have been a random distribution of such fibers that happen to be located at the edges.

Fiber Surface Morphology. Representative results from the multiple images taken of aramid fibers before and after mixing are shown in Figures 8 and 9. Aramid are highly oriented aromatic polyamides, which presents challenges in creating fibers. The process of wet-spinning is typically adopted and yields a fiber with very high strength along the axis of the fiber, but made up of many layers bonded together with relatively low strength (*15*). As a result, during agitation the surface of the aramid fibers may fibrillate into strands that effectively increase the bonding area of the fiber resulting in increase of pull-out resistance.

Figures 8*c* and 9*b* show the surfaces of the clustered fibers and again they appear much the same with only slightly greater surface fibrillation. However, the images from individual condition showed a different morphology, Figures 8*d* and 9*c*. In these fibers, micro-fibrillation is apparent. Although it is not quantified, it also appears that the individual fibers from FA are more fibrillated than FB. This effect may occur because the fibers disperse more quickly in FA and are therefore agitated in the individual condition for a longer time compared with the wax coating on FB. The significance of this effect is that not all individual fibers have the same state even though they may be dispersed and distributed in the same way.

Figure 8*a* shows the fibers in their original condition and it is seen that each fiber is cylindrical and 10–14 μm long in diameter. Most of the fibers are smooth, with a few occasional micro-fibrillations (circled in red). These fibrillations are approximately 0.5–2 μm wide and 35–150 nm thick. In Figures 8*b–d* and 9*a–c*, small dots appear on the surface of the fibers, which are leftover dust from the extraction and cleaning process. Figures 8*b* and 9*a* show the surface of the agitated bundles, and it is seen that the fibers retain much of the same morphology as the unagitated bundles.

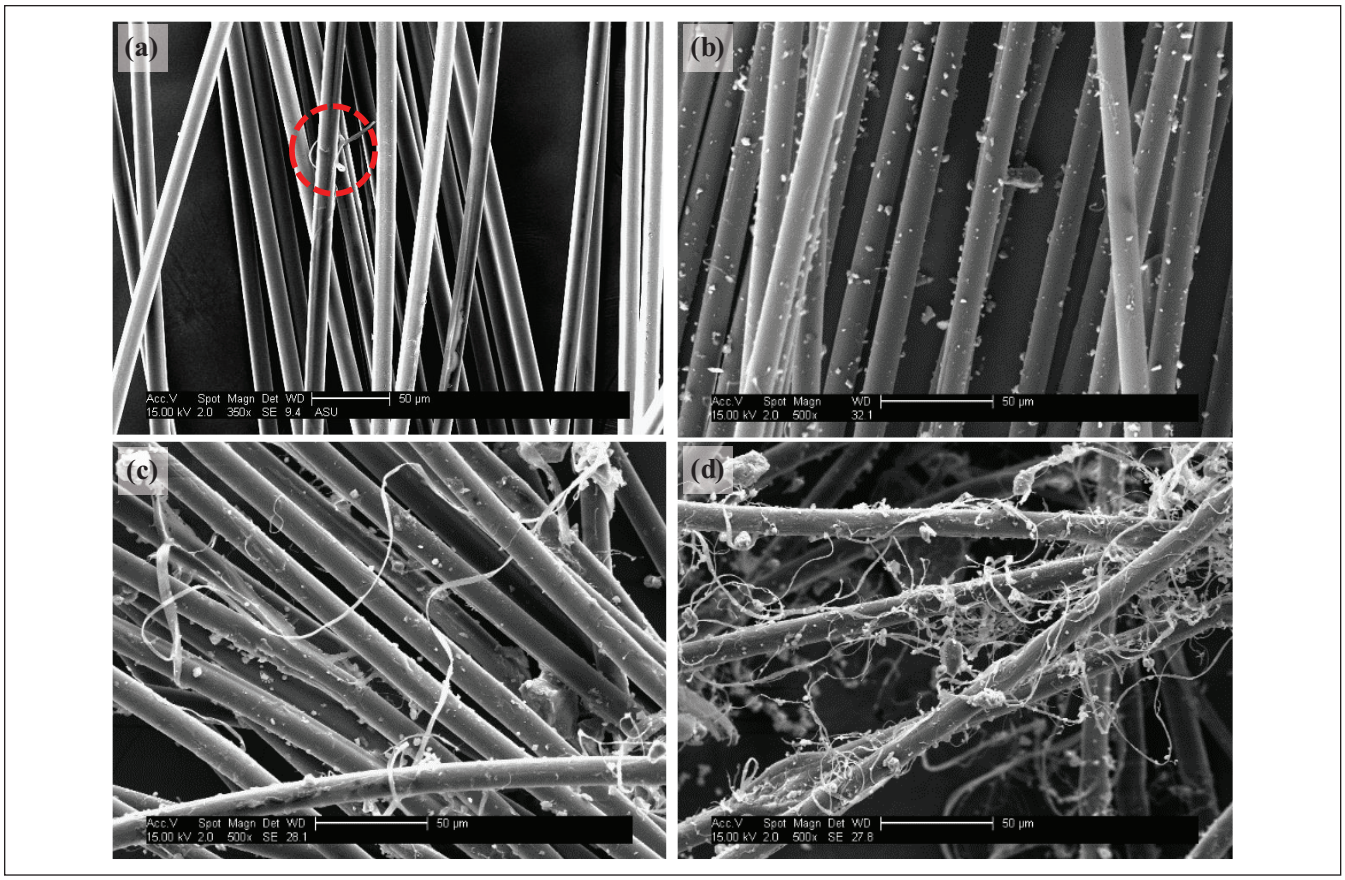

Figure 8. SEM images of aramid fibers of FA mix at different conditions: (*a*) original bundles (unagitated), (*b*) extracted agitated bundles, (*c*) extracted clusters, and (*d*) extracted individual fibers (all images at 500× magnification).

Discussion

In this study, the repeated load permanent deformation test showed improved performance in FA mixture over FB and control mixtures. Since both FA and FB mixtures contained aramid fibers at the same volumetric content but yielded different behaviors, it can be inferred that volumetric content alone is not a sufficiently descriptive metric to quantify fibers in M-FRAC. The fact that FA exhibits substantially less permanent strain accumulation and has a larger flow number, along with the fact that the fibers in FA were more dispersed, distributed, and fibrillated, may suggest that additional fiber metrics play a role in the fibers' effectiveness. From the improved permanent deformation test results and in light of the orientation findings, it is theorized that the fibers function, as they do in other composites, by bridging or reinforcing cracks. In this case horizontal cracks are developed during the flow number test. In this theory, it is postulated that a more dispersed and distributed fiber system acts to reinforce more flaws and thus more greatly improve the performance. It is also possible that the effectiveness of the fibers in bridging cracks is aided by micro-fibrillation of the fiber surfaces, although this is not verified in any way here. A higher level of this micro-fibrillation would mean a higher surface area of fibers in the matrix and a stronger overall bond.

Additional insights are gained by considering the fatigue tests. Here, both FA and FB showed improvement over the control, but there was no discernable difference between the two M-FRAC mixtures. The combined fatigue and permanent deformation behaviors are attributed to the same phenomenon, which is that the individual aramid fibers in these mixtures tended to orient perpendicular to compaction. In this configuration, the fibers are ideally oriented to reinforce cracks that form parallel to the loading direction (as in compression loading), but are not ideally oriented for reinforcing cracks developing perpendicular to the loading direction (as in tension loading). Since the agitated bundles are not well distributed, their effectiveness is reduced. While they may reinforce cracks, they are only located in a few places and so the overall role of this reinforcement on the continuum is apparently small. Stated differently, a well-distributed network of fiber reinforcement in the proper directions is necessary since failure can occur on any plane. A large volume of the material left unreinforced can dictate the overall performance of the material. This study does not identify a critical threshold of individual fibers needed to achieve an effective

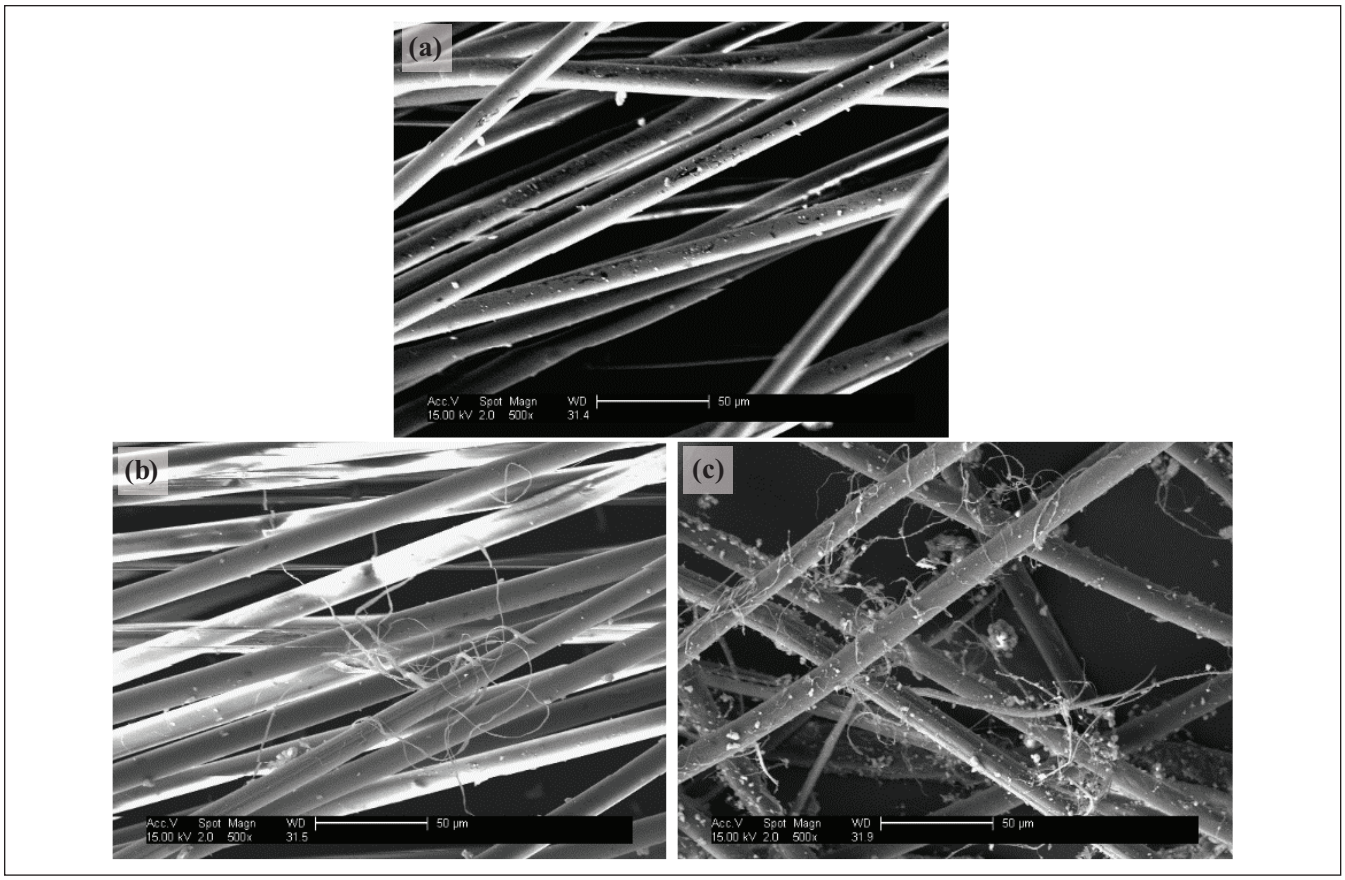

Figure 9. SEM images of extracted aramid fibers of FB mix at different conditions: (*a*) agitated bundles, (*b*) clusters, and (*c*) individual fibers (all images at 500× magnification).

network. It can only be stated that this threshold is somewhere between an *ADSR* of 16% (that from FB) and an *ADSR* of 88.5% (that from FA). Whether this network formation follows a simple linear, nonlinear, or percolation type relationship cannot be determined from the current data.

Finally, it should be stated that the orientations of the fibers with respect to the testing configuration in this study is a direct result of the laboratory fabrication procedure. The evaluation of field cores was beyond the scope of this study but would provide additional insights. Here the gyratory compactor is used to create specimens by compacting them along the same direction that the major principal stress is applied during tests. In the case of compression, these orientations generally align with pavement construction and vehicular loading. However, in tension these orientations differ since tension in a pavement is induced in a direction perpendicular to the compaction direction. Failure to consider these differences may lead to laboratory results that underestimate the true fatigue benefits from M-FRAC mixtures. Also, the study findings are isolated to the single mixture studied, and additional testing incorporating more careful documentation of fiber state is warranted in order to refine the theory further. What this study does demonstrate is that understanding M-FRAC benefits can be improved by considering the state of the fiber within the mixture.

Conclusion

This paper has investigated how the state of aramid fibers would influence the mechanical properties of asphalt mixtures. The following conclusions were reached in this study.

- Dynamic moduli values showed no statistical differences between the three mixtures.
- The FA mixture exhibited a 139% improvement in flow number compared with the control while the FB mixture had a similar performance to the control mixture.
- Fatigue simulations showed that both FA and FB mixtures had two times fatigue improvement compared with the control.
- Aramid fibers in FA mix were well dispersed and most of the fibers were in the individual state (*ADSR* of 88.5%) while FB fibers were poorly dispersed (ADSR of 16%).
- FA and FB specimens showed even distribution of the fibers in the individual fiber state but also a higher

number of individual fibers on the surface of FA specimens. Besides, it was observed that individual fibers tend to be oriented mostly horizontally.

- Aramid fibers in FA mix showed a higher degree of micro-fibrillation compared with aramid fibers in FB mix.
- The different behavior in fatigue and permanent deformation for each FA and FB was attributed to the orientations of the fibers with respect to the testing configuration. It was postulated that in the flow number test the fibers are ideally oriented to strengthen cracks that form parallel to the loading direction, whereas fibers are not preferably oriented for reinforcing cracks that develop perpendicular to the loading direction in the fatigue test.

Author Contributions

The authors confirm contributing to the paper as follows: study conception and design: Hossein Noorvand, B. Shane Underwood; data collection: Hossein Noorvand, Ramadan Salim, Jose Medina; analysis and interpretation of results: Hossein Noorvand, B. Shane Underwood; draft manuscript preparation: Hossein Noorvand, B. Shane Underwood, Jeffrey Stempihar. All authors reviewed the results and approved the final version of the manuscript.

References

1. Mcdaniel, R. *Fiber Additives in Asphalt Mixtures*. Transportation Research Board of the National Academies, Washington, D.C., 2015.
2. Abtahi, S. M., M. Sheikhzadeh, and S. M. Hejazi. Fiber-Reinforced Asphalt-Concrete – A Review. *Construction and Building Materials*, Vol. 24, No. 6, 2010, pp. 871–877.
3. Huang, H., and T. White. Dynamic Properties of Fiber-Modified Overlay Mixture. *Transportation Research Record: Journal of the Transportation Research Board*, 1996. 1545: 98–104.
4. Mcdaniel, R., and A. Shah. *Asphalt Additives to Control Rutting and Cracking*. Publication FHWA/IN/JTRP-2002/29. Joint Transportation Research Program, Indiana Department of Transportation and Purdue University, West Lafayette, 2003.
5. Behbahani, H., S. Nowbakht, H. Fazaeli, and J. Rahmani. Effects of Fiber Type and Content on the Rutting Performance of Stone Matrix Asphalt. *Journal of Applied Sciences*, Vol. 9, No. 10, 2009, pp. 1980–1985.
6. Kaloush, K. E., K. P. Biligiri, W. A. Zeiada, M. C. Rodezno, and J. X. Reed. Evaluation of Fiber-Reinforced Asphalt Mixtures Using Advanced Material Characterization Tests. *Journal of Testing and Evaluation*, Vol. 38, No. 4, 2010, pp. 400–411.
7. Tapkın, S. The Effect of Polypropylene Fibers on Asphalt Performance. *Building and Environment*, Vol. 43, No. 6, 2008, pp. 1065–1071.
8. Lee, S. J., P. J. Rust, H. Hamouda, Y. R. Kim, and R. H. Borden. Fatigue Cracking Resistance of Fiber-Reinforced Asphalt Concrete. *Textile Research*, Vol. 75, No. 2, 2005, pp. 123–128.
9. Maurer, D. A., and G. J. Malasheskie. Field Performance of Fabrics and Fibers to Retard Reflective Cracking. *Geotextiles and Geomembranes*, Vol. 8, No. 3, 1989, pp. 239–267.
10. Simpson, A. L, and M. C. Case Study of Modified Bituminous Mixtures: Somerset, Kentucky. *Proc., 3rd Materials Engineering Conference, San Diego, CA, ASCE*, New York, 1994, pp. 88–96.
11. Xu, Q., H. Chen, and J. A. Prozzi. Performance of Fiber Reinforced Asphalt Concrete Under Environmental Temperature and Water Effects. *Construction and Building Materials*, Vol. 24, No. 10, 2010, pp. 2003–2010.
12. Mobasher, B. *Mechanics of Fiber and Textile Reinforced Cement Composites*. CRC Press, Boca Raton, Fla., 2011.
13. Underwood, B., C. Baek, and Y. Kim. Simplified Viscoelastic Continuum Damage Model as Platform for Asphalt Concrete Fatigue Analysis. *Transportation Research Record: Journal of the Transportation Research Board*, 2012. 2296: 36–45.
14. Zeiada, W., J. Medina, S. Underwood, and J. Stempihar. *Fiber-Reinforced Asphalt Concrete Laboratory Procedure: Verification of Aramid Dispersion*. Forta Corporation, Grove City, PA 2017.
15. Hahn, C. Characteristics of P-aramid Fibers in Friction and Sealing Materials. *Journal of Industrial Textiles*, Vol. 30, No. 2, 2000, pp. 146–165.

The Standing Committee on Non-Binder Components of Asphalt Mixtures (AFK30) peer-reviewed this paper (18-05606).